Pure & Appl. Chem., Vol. 63, No. 2, pp. 243–254, 1991.
Printed in Great Britain.

206922209100027

Gas-phase reactivity of five-membered heteroaromatics toward electrophiles, an experimental check on theoretical predictions

Maurizio Speranza

Dipartimento di Agrobiologia ed Agrochimica, Università della Tuscia, Viterbo, Italy.

Abstract. Pyrrole, N-methylpyrrole, furan, and thiophene have been first employed as model structures for a comprehensive evaluation of heteroaromatic reactivity in the gas phase, where complications due to the solvent, catalyst, counterion, etc., are minimized. Under such conditions, direct evaluation of the intrinsic reactivity properties of the selected heteroarenes is allowed and gas-phase kinetic data can be used with some confidence for testing the validity of the most advanced reactivity models, including Klopman's Charge and Frontier Orbital Control concept and Shaik and Pross' Curve Crossing model. On the basis of the quality of the correlations between the experimental kinetic data and the energy gap between the unperturbed orbitals of the donor and the acceptor, which in both models is a major factor determining reactivity, it emerges that Klopman's approach to the description of the gas-phase reactivity of heteroarenes toward ionic electrophiles can be thought as a special case of the more general Curve Crossing model. A quantitative application of Shaik and Pross' approach allowed to rationalize intrinsic heteroaromatic reactivity in terms of physically meaningful quantities, namely the vertical ionization potential of the donor and the vertical electron affinity of the acceptor.

INTRODUCTION

Electrophilic substitution of five-membered heteroaromatic rings is a challenging area within which the modern concepts of theoretical chemistry and chemical reactivity find not only their widest application but also their inherent limits. Despite intense kinetic and mechanistic investigations, very few quantitative data are available that allow for a direct evaluation of the reactivity scale of simple heteroaromatics. The data accumulated show that, in solution, heteroaromatic reactivity may span over many orders of magnitude with the sequential hierarchy : N-methylpyrrole > pyrrole >> furan > thiophene > benzene (ref. 1). However, no reasonable explanation for this behavior has been so far presented . Certainly, environmental factors play a decisive role in determining such a large reactivity difference. The current literature of the field is studded with evidence for profound environmental effects on the magnitude of simple physical properties of fundamental heteroaromatics that are related to their electron density distribution (*e.g.* the overall dipole moment). These physical alterations are reflected in dramatic effects of the reaction medium upon the reactivity features of the heteroaromatic compounds. As a consequence, most of the heteroaromatic reactivity scales from solution studies are devoid of any quantitative significance since they originate from kinetic measurements carried out under diverse environmental conditions (refs. 1 and 2). Environmental factors often determine the directive properties of a given heteroaromatic ring toward electrophilic attack as well, although α substitution appears to be a general rule in the condensed phase.

A radical solution to all the above-mentioned difficulties is to eliminate the solvent medium entirely and to measure structural effects on heteroaromatic reactivity in the gas phase (ref. 3). During the last decade, a revolution has occurred in the experimental and theoretical approaches to understanding gas-phase ion chemistry. This is the consequence of the simultaneous development of several experimental methods for studying organic ion-molecule kinetics and equilibria in the gas phase with precision and range of effects equivalent to or even better than that normally obtained in solution and by very sophisticated molecular orbital calculations. The importance of reactivity studies in the gas phase is twofold. Direct comparison of rates and equilibria in gaseous and condensed media reveals previously inaccessible effects of ion solvation. In addition, reactivity data in the gas phase provide a direct evaluation of the fundamental, intrinsic properties of molecules and represent a unique yardstick against which the validity of theoretical estimates of such properties can be adequately assayed.

Achievement of this goal is within the reach of recently developed radiolytic and nuclear-decay techniques that allow for the kinetic analysis of gas-phase ionic reactions by the same methodology typical of solution chemistry, based *inter alia* on the actual isolation of the neutral end products and the determination of their isomeric composition. By either procedure, a variety of free, unsolvated ionic electrophiles of well defined structure and energy, *i.e.* CH_3^+, $C_2H_5^+$, i-$C_3H_7^+$, t-$C_4H_9^+$, $(CH_3)_3Si^+$, $(CH_3)_2F^+$, $C_6H_5^+$, CH_3CO^+, $C_6H_5CO^+$, and CF_3^+, have been generated in the gas phase and allowed to react with representative five-membered heteroarenes, such as pyrrole, N-methylpyrrole, furan, and thiophene, under kinetically controlled conditions.

In this report, a first, homogeneous set of kinetic data concerning the intrinsic reactivity of the selected heteroarenes is presented and used for testing the predictive value of most refined reactivity models, including Klopman's Charge and Frontier Orbital Control concept and Shaik and Pross' Curve Crossing model.

METHODOLOGIES

The radiolytic technique is based on the generation of unsolvated ions by the passage of high-energy electromagnetic radiation (X or γ rays) through the gaseous system (ref. 4). High-energy quanta lose energy to the medium through photoelectric and Compton effects, or *via* pair-production processes, which ultimately result in the release of energetic (up to hundreds of eV) electrons, responsible for more than 99% of the ionization and excitation events in the irradiated gas. The fate of the reactive species formed (ions, electrons, radicals, and excited molecules) can be controlled to a certain extent by the composition of the irradiated system. Thus excited species can be made to lose their excess energy *via* many unreactive collisions with the bath gas, *i.e.* the major component of the gaseous system. Their thermalization takes place prior to reaction with the neutral substrate of interest present in the gas at very low concentrations (*e.g.* 0.1 mol%). Undesired radical reactions can be efficiently suppressed by appropriate radical scavengers, which nevertheless must be inert toward the ionic species investigated (*e.g.* O_2). The actual isolation of the neutral products from the ionic processes occurring in the irradiated mixture and the determination of their structure and isomeric composition, in terms of the experimental conditions, provide useful and otherwise inaccessible information regarding the gas-phase reactivity of the neutral substrates investigated toward the radiolytically formed ionic reactants. By this procedure, $C_2H_5^+$ (ref. 5), i-$C_3H_7^+$ (ref. 6), t-$C_4H_9^+$ (ref. 7), $(CH_3)_3Si^+$ (ref. 8), $(CH_3)_2F^+$ (ref. 9), CF_3^+ (ref. 10), and CH_3CO^+ (ref. 11) have been generated respectively from CH_4, C_3H_8, neo-C_5H_{12}, $CH_4/(CH_3)_4Si$, CH_3F, CF_4, and CH_3F/CO mixtures and their reactivity toward the selected heteroarenes evaluated.

The nuclear-decay technique is based on the spontaneous decay of a tritium atom covalently bound in an appropriate precursor (ref. 12). The nuclear transition in the tritium atom of a tritiated molecule RT gives stable ^3He and R^+ daughters *via* emission of an antineutrino and a β particle, whose energy ranges up to *ca.* 18 keV, with a mean value of 5.6 keV. The chemical consequences of the β decay arise in part from the excitation of the daughter species because of the momentum imparted to the ^3He moiety following emission of the β and ν particles and the perturbation ("shaking") of the electron cloud after the sudden increase of the nuclear charge (ref. 13). Theoretical treatments predict and sophisticated mass-spectrometric experiments confirm that such recoil and electronic excitation sources may cause fragmentation and multiple ionization only in a small fraction (10-20%) of the primary decay species, whereas the remainder (90-80%) is formed in the ground state, with negligible recoil and excitation energy. An additional source of excess internal energy of ground-state R^+ is the deformation energy associated with its "wrong" geometry. If fact, the decay event in RT occurs in a time far too short to allow relaxation of the structure typical of the neutral parent (*e.g.* the tetrahedral CH_3T) to the most stable geometry of the daughter ion (*e.g.* the planar CH_3^+). Such a "deformation energy" has been calculated around 30 kcal mol^{-1} for methyl cation from tritiated methane and for the phenylium ion from the decay of tritiated benzene (ref. 14). By this approach, $C_6H_5^+$ (ref. 15), $C_6H_5CO^+$ (ref. 11), and CH_3^+ (ref. 16) have been generated under largely different experimental conditions, from the dilute gas state to dense gases to liquids, from nuclear-decay in multitritiated benzene, benzene/CO, and methane precursors, respectively, and their reactivity toward the selected heteroarenes investigated. Standard quantum-mechanical calculations, with the GAUSSIAN 80 (ref. 17) set of programs, were performed in order to evaluate the SCF STO-3G and 6-31G* (ref. 18) eigenvalues of the LUMO's of CH_3^+, $C_2H_5^+$, i-$C_3H_7^+$, t-$C_4H_9^+$, $(CH_3)_3Si^+$, $(CH_3)_2F^+$, CF_3^+, $C_6H_5^+$, CH_3CO^+, and $C_6H_5CO^+$, and of the HOMO of pyrrole. Geometry optimizations were performed in order to obtain the SCF STO-3G and 6-31G* optimized wave functions and orbital eigenvalues. D_{3h} symmetry was assumed for CH_3^+ and CF_3^+, C_{3v} for t-$C_4H_9^+$ and $(CH_3)_3Si^+$, and C_{2v} for

i-$C_3H_7^+$, $C_6H_5^+$, CH_3CO^+, $C_6H_5CO^+$, $(CH_3)_2F^+$, and pyrrole. The computed LUMO eigenvalues at the SCF STO-3G level of theory are as follows (in eV) : CH_3^+ (-6.36, ground state; -7.36, vibrationally excited), $C_2H_5^+$ (-1.92, proton-bridged structure), i-$C_3H_7^+$ (-3.90), t-$C_4H_9^+$ (-3.13), CF_3^+ (-5.19), $C_6H_5^+$ (-3.51, ground state; -5.50, vibrationally excited), CH_3CO^+ (-2.43), $C_6H_5CO^+$ (-2.36), $(CH_3)_3Si^+$ (-1.78), and $(CH_3)_2F^+$ (+1.77). The calculated HOMO eigenvalue for pyrrole at the same level of theory is -6.64 eV. The computed LUMO eigenvalues at the SCF 6-31G* level of theory are as follows (in eV): CH_3^+ (-7.63, ground state; -8.63, vibrationally excited), $C_2H_5^+$ (-3.79, proton-bridged structure; -6.19, open structure), i-$C_3H_7^+$ (-5.10), t-$C_4H_9^+$ (-4.42), CF_3^+ (-7.24), $C_6H_5^+$ (-4.96, ground state; -6.46, vibrationally excited state), CH_3CO^+ (-3.46), $C_6H_5CO^+$ (-3.51), and $(CH_3)_3Si^+$ (-4.19). The calculated HOMO eigenvalue for pyrrole is -7.96 eV.

RESULTS

The relative yields of the substituted products from the gas-phase attack of the selected ionic electrophiles on pyrrole and furan are given in Figure 1. Inspection of Fig. 1 reveals that the major part of the selected electrophiles, *i.e.* $C_2H_5^+$, i-$C_3H_7^+$, t-$C_4H_9^+$, $(CH_3)_3Si^+$, and $(CH_3)_2F^+$, attacks preferentially the β carbons of pyrrole (>70%). On the contrary, CH_3^+, $C_6H_5^+$, and acylium ions display a pronounced affinity for the α positions of the same substrate (>72%). The CF_3^+ ions appear rather unselective toward the C centers of pyrrole with a slight preference for the β positions (56%). A temperature-dependence study of the site selectivity of several of these ions, *i.e.* i-$C_3H_7^+$, t-$C_4H_9^+$, CF_3^+, $(CH_3)_2F^+$, and CH_3CO^+, toward gaseous pyrrole has been undertaken with the aim of estimating the activation parameters governing the relevant substitution reactions. The experiments have been carried out under kinetically controlled conditions, *i.e.* at atmospheric pressure and in the presence of 2 torr of the powerful base NMe_3, within the temperature interval from 30 to 140°C. The results are plotted in Figure 2. The Arrhenius plots relative to CF_3^+, CH_3CO^+, and $(CH_3)_2F^+$ are linear over the entire temperature interval, while those relative to i-$C_3H_7^+$ and t-$C_4H_9^+$ are characterized by a marked inflection above 110 and 70°C, respectively, due to the occurrence of appreciable proton transfer process to pyrrole above those temperatures. Besides, while Arrhenius curves for alkyl cations display a distinct negative temperature dependence, that concerning the halonium ion $(CH_3)_2F^+$ is characterized by the reverse trend. Finally, no significant temperature effects are observed as regard to the site selectivity of acetyl cation toward gaseous pyrrole.

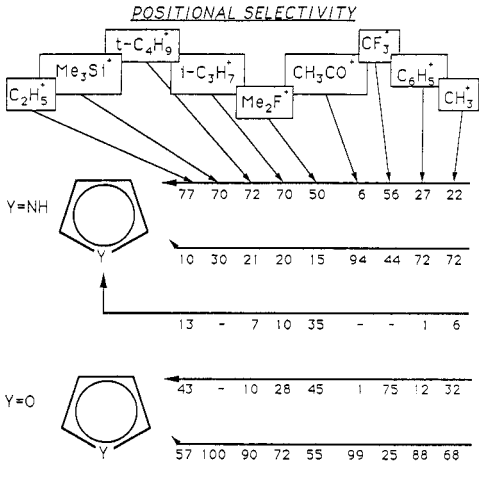

Fig. 1. Positional selectivity of the selected ionic electrophiles toward pyrrole and furan.

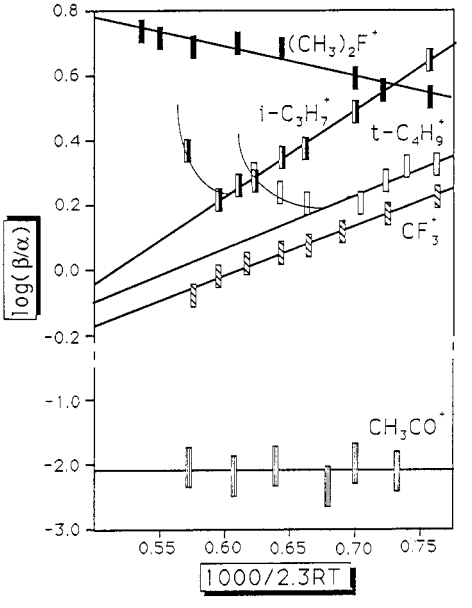

Fig.2. Arrhenius plots for the competitive attack of ionic electrophiles toward the β and α carbons of pyrrole.

Furan undergoes predominant substitution at its α centers by all selected electrophiles (>55%), except CF_3^+ (25%). Experimental evidence for significant attack at its oxygen atom is achieved as well. N-methylpyrrole displays orienting properties similar to those of pyrrole, whereas thiophene is characterized by predominant α substitution from all electrophiles employed. The pronounced site selectivity of the ionic reactants strikingly contrasts with their very limited substrate selectivity, as measured from competition experiments carried out using toluene as the reference substrate under kinetically controlled conditions. As an example, the apparent rate constant relative to toluene for methylation by $(CH_3)_2F^+$ is found to decrease in the order : furan (1.7) > N-methylpyrrole (1.4) > thiophene (1.1) > pyrrole (0.6), namely with the dipole moment and the polarizability of the substrate, in fair agreement with current theories on ion-molecule interactions in the gas phase (ref.19).

DISCUSSION

The essence of Klopman's Charge and Frontier Orbital Control concept (ref. 20) in a donor-acceptor reaction is that, when the energy gap between the HOMO of the donor and the LUMO of the acceptor is small compared to that between the orbitals of the individual reagents, the reaction is "frontier-orbital controlled", *i.e.* it is governed by bonding between the atoms carrying the highest charge density in the frontier orbital. When, instead, the energy gap between the HOMO of the donor and the LUMO of the acceptor progressively increases, the reaction tends to be "charge-controlled", *i.e.* it is regulated by attractive electrostatic interactions between the centers of the two reagents with the highest total charge. If the acceptor is a free, unsolvated ionic electrophile and the donor is a five-membered heteroarene, such as pyrrole or furan, having a HOMO electron density distribution opposite to the total charge-density one (Figure 3) (ref. 3), a comparison between the intrinsic reactivity and selectivity features of the ionic electrophiles toward these substrates and their calculated LUMO energies may represent a powerful means for ascertaining whether Klopman's model is actually adequate for describing heteroaromatic reactivity, especially if the reactivity data refer to gas-phase processes, where solvation and ion-pairing factors normally affecting the intrinsic properties of both the donor and the acceptor are excluded. Figure 4 shows that an approximately linear correlation actually exists between the site selectivity of the selected electrophiles toward pyrrole (log(β/α) and their SCF STO-3G calculated LUMO energy (ε(LUMO)), in qualitative agreement with Klopman's predictions. In fact, ionic electrophiles with high-energy LUMO's are electrostatically directed toward the ring carbons of

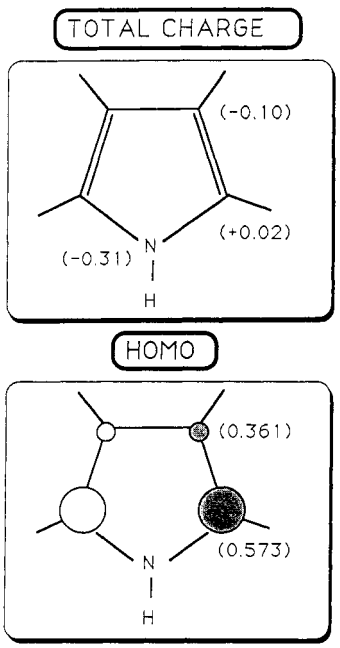

Fig. 3. First HOMO electron density and charge density distribution in pyrrole.

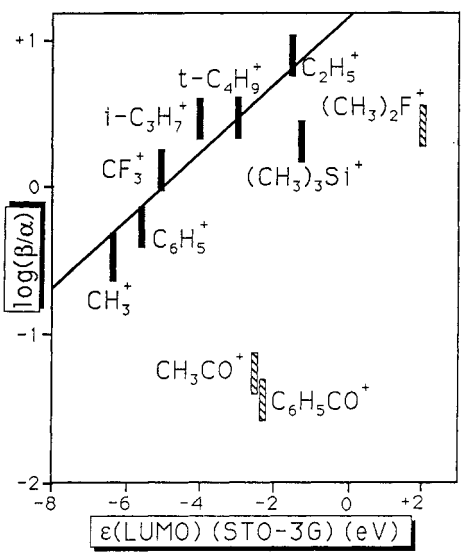

Fig. 4. Plot of site selectivity of ionic electrophiles toward the β and α carbons of pyrrole, expressed by the log(β/α), as a function of SCF STO-3G calculated LUMO eigenvalues of the selected ionic electrophiles.

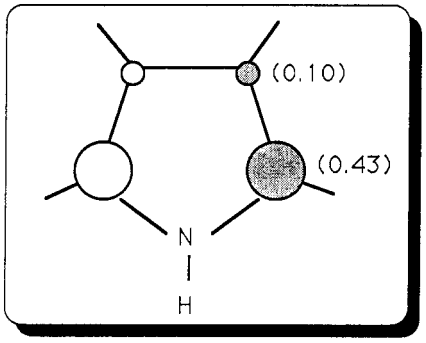

Fig. 5. Spin density distribution in carbon 2p π orbitals of pyrrole radical cation.

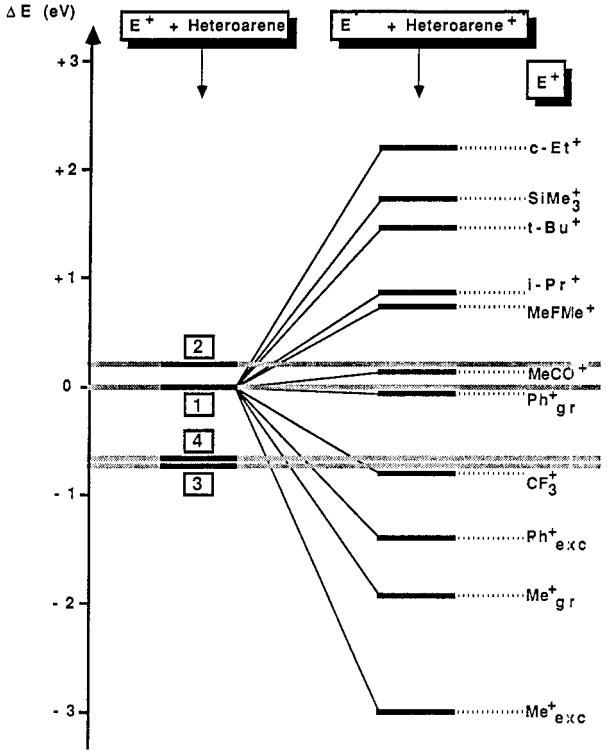

Fig. 6. Energetics of the vertical electron transfer from simple five-membered heteroarenes (pyrrole (1), N-methyl pyrrole (2), furan (3), thiophene (4)) to the electrophile E^+. The $EA_v(E^+)$ is expressed approximately by $-IP_a(E\cdot)$.

pyrrole with the highest net negative charge, *i.e.* the β carbons (*e.g.* t-$C_4H_9^+$ (ε(LUMO) = -3.1 eV); log(β/α) = 0.54) (ref. 7), whereas ionic reactants with low-energy LUMO's preferentially establish partial electron exchange with the ring centers of the same heteroarene with the highest HOMO π-electron density, *i.e.* the α carbons (*e.g.* CH_3^+ (ε(LUMO) = -6.4 eV); log(β/α) = -0.51) (ref. 16). A similar correlation is obtained by upgrading to 6-31G* the level of calculation of the frontier orbital energies of the donor-acceptor pair. For N-methylpyrrole, a correlation similar to that of Fig. 4 is obtained as well.

However, when unsaturated carbocations, such as acylium, phenylium , and dimethylfluoronium ions are considered, appreciable deviations from the linear correlation are observed, reflecting a measured positional selectivity toward pyrrole well below that expected on the grounds of their STO-3G calculated LUMO energies (ε(LUMO) (eV) = -2.4 (acylium ions); -3.5 (ground-state phenylium ion); -5.5 (vibrationally-excited phenylium ion); +1.77 (dimethylfluoronium ion).

The exceedingly large predominance of α substitution displayed by acylium ions and its scarce sensitivity to even large temperature variations (30-140°C) (Fig. 2) are consistent, in compliance with independent FT-ICR mass spectrometric evidence, with a gas-phase acylation reaction toward pyrroles proceeding *via* a quasi-resonant single-electron transfer (SET) step followed by recombination between the ensuing acyl radical and the ring positions of the pyrrole radical-ion having the highest spin density, *i.e.* the α carbons (ref. 21) (Figure 5).

Kinetic predominance of the two-steps substitution sequence over the classical donor-acceptor S_E2 mechanism in the attack of gaseous acylium ions on heteroarenes is determined by both favorable entropy factors and limited activation barriers, in view of the energetically quasi-resonant character of the vertical SET process from the heteroarene to the acylium ion (Figure 6). For all the other electrophiles, for which such a condition is inaccessible, the S_E2 mechanism prevails over the alternative SET process, as evidenced by the correlation of Fig. 4.

The nature of the employed electrophiles, *i.e.* free, unsolvated carbenium and halonium ions, as well as the gaseous reaction environment, which excludes interference from solvation and ion-pairing phenomena, confers to the present experimental results an unusual degree of generality and of relevance for comparison with current reactivity theories, such as Klopman's model.

Klopman's concept of charge *vs.* orbital control in a donor-acceptor reactions, as determined by the energy level, the shape, and the charge distribution of the *unperturbed* HOMO of the donor and of the LUMO of the acceptor, is recognized, on the basis of the correlations of Fig. 4, as a qualitative model for electrophilic heteroaromatic reactivity in the gas phase. Nevertheless, it appears inherently inadequate for a quantitative description of the heteroaromatic reactivity in the gas phase, which is based upon a kinetic evaluation of the relevant potential energy hypersurfaces, determined by the *mutual perturbation* of the orbitals of the donor and of the acceptor along the reaction coordinate. An enlightening example is provided by the activation parameters obtained from regression analysis of the data in the linear portions of the Arrhenius plots of Fig. 2 ($\Delta E^* = E^*_\alpha - E^*_\beta$ (in kcal mol $^{-1}$) = +2.1 (t-$C_4H_9^+$); +2.9 (i-$C_3H_7^+$); +1.8 (CF_3^+); -1.0 ($(CH_3)_2F^+$); $\log(A_\beta/A_\alpha)$ = -1.1 (t-$C_4H_9^+$); -1.5 (i-$C_3H_7^+$); -1.1 (CF_3^+); +1.3 ($(CH_3)_2F^+$). Another is the reversal of the positional selectivity of gaseous CF_3^+ toward pyrrole as a function of the temperature (Fig. 2). Both cannot find any rationalization on the exclusive grounds of Klopman's concept, but call for a quantitative application of more refined models, such as the Curve Crossing model by Shaik and Pross (ref. 22), which anchors the theoretical treatment of the experimental kinetic data to factors determining the activation barriers in a typical donor-acceptor reaction.

The Quantitative Curve-Crossing Model for Heteroaromatic Reactivity in the Gas Phase. The essence of the Curve-Crossing model is to use electronic configurations of the reactants and of the products as building blocks from which the entire energy profile along a reaction coordinate may be generated. For donor-acceptor reactions, such as those considered in the present study involving a neutral pyrrole nucleophile (**Nu:**) and a cationic electrophile (E^+), the reactant configuration is depicted by the **Nu:**/E^+ pair, while the configuration that describes the substituted heteroarenium product is depicted by $Nu^{\cdot+}$/$E^{\cdot}$. It can be seen that all that is required to convert the reactant pair into the heteroarenium product is a *formal* single electron transfer from **Nu:** to E^+, described by the **Nu:**/E^+ - $Nu^{\cdot+}$/$E^{\cdot}$ configuration mixing along the reaction coordinate. In the framework of the Valence-Bond Configuration Mixing (VBCM) model (ref. 22b), the electrophilic attack of a cation E^+ on pyrrole **Nu:** can be conceived as involving essentially the lowest-energy empty orbital of E^+ and the formally localized substituted C=C π bond of pyrrole **Nu:**. This latter is obtained by deconvoluting the delocalized molecular π orbitals of pyrrole into the localized ones. In this way, a pyrrole molecule can be treated as an enamine molecule, whose π orbital is the one obtained by the pyrrole molecular π–orbitals localization procedure.

In this view, the active configurations **I**-**III** (Figure 7) must be employed to build up the adiabatic potential energy profile for the electrophilic addition of E^+ to pyrrole. In Fig. 7, the origin of the vertical axis, reporting the energy of the reactant and the product configurations in eV, is taken as the absolute energy of the **Nu:**/E^+ configuration **I**. The horizontal axis refers to the distance **r** (in Å) between the positively charged center of E^+ and the C atoms of **Nu:**. This parameter is assumed as the reaction coordinate, and its zero-value is taken at a real distance between E^+ and **Nu:** of 4.1 Å, which is the minimum distance whereto C-C orbital overlap is still negligible (see Fig. 8). As can be observed from Fig. 7, two different product configurations of $Nu^{\cdot+}$/$E^{\cdot}$, *i.e.* **II** and **III**, must be considered, the first with an electron vacancy at the β carbon of pyrrole, collapsing eventually to the α-substituted heteroarenium product, and the other with an electron vacancy at the α carbon of the nucleophile, leading to the β-substituted heteroarenium isomer. As a first approximation, only one reactant configuration, *i.e.* **I**, involving the localized π orbital of pyrrole can be assumed. Besides, in order to make quantitatively tractable the kinetic data of Fig. 4 in the framework of the Curve Crossing model, a linear dependence of the energy of each configuration, at least for a limited range of the reaction coordinate, is assumed.

For the donor-acceptor reaction described in Fig. 7, the initial energy gap **G** between configurations **I** and **II** will be given by the difference between the vertical ionization potential of **Nu:** (IP_V(**Nu:**)) and the vertical electron affinity of E^+ ($EA_V(E^+)$), which represents approximately the energy necessary to transfer vertically an electron from the β carbon of the donor **Nu:** to the acceptor E^+. If, instead, the transition involves configuration **III**, with the electron vacancy at the α carbon of the donor, the configuration energy gap is represented by the **G**+δ

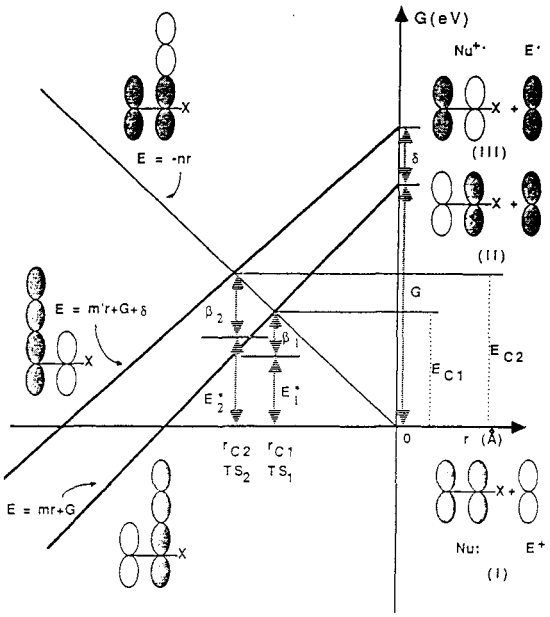

Fig. 7. State correlation diagram for a Nu:/E+ donor-acceptor reaction representing a typical gas-phase heteroaromatic substitution by an ionic electrophile.

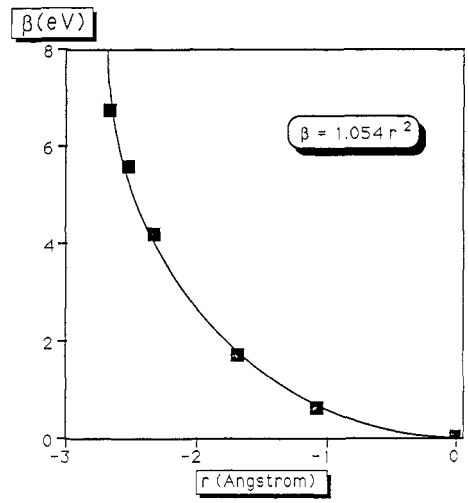

Fig. 8. Best-fit parabolic equation representing the dependence upon the reaction coordinate **r** of the resonance integral β between 2p orbitals of interacting carbon atoms.

term, where δ is the energy gap between **II** and **III**. In view of the predominant spin-density localization at the α carbons of pyrrole radical cation (ref. 21), a positive value for the energy parameter δ is expected.

The equation **E(I) = -nr**, with **n > 0**, describes the dependence of the energy of the reactant configuration upon the reaction coordinate **r**. The curves reporting the energy of the product configurations **II** and **III** as a function of **r** obey the following equations: **E(II) = mr+G** and **E(III) = m'r+G+δ**, respectively. In order to build up the entire potential energy profile, the interaction of the involved configurations at any point of the reaction coordinate must be allowed.

From the perturbation theory (ref. 23), this interaction involves a stabilization energy **SE** relative to the energy of the most stable of the interacting configurations, which is expressed by $SE = \beta^2/\Delta E$, where **ΔE** represents the energy gap between the two interacting configurations along the reaction coordinate and β is an energy parameter. At the curve-crossing point, where the interacting configurations become degenerate at an energy value of E_C, the stabilization energy is simply equal to β. Here, the reaction coordinate r_C is that of the transition state, whose energy **E*** can be therefore estimated from the E_C-β difference. Being referred to the energy of the unperturbed reactant configuration, taken equal to zero, $E^* = E_C - \beta$ represents the activation energy of the process. For the interaction of two configurations, such as for instance **I** and **II**, which are related by a *formal* single electron transfer, the magnitude of β is essentially proportional to the overlap between the two atomic orbitals which differ in one-electron occupancy (ref. 24).

Since, in our case, most of the atomic orbitals involved in the *formal* electron transfer are 2p's of carbon, the resonance integral β can be described satisfactorily by the equation $\beta = \kappa r^2$, with $\kappa = 1.054$ eV Å^{-2}, which is found to be the best interpolating parabolic function (Figure 8; correlation coefficient = 0.994), expressing the dependence of the calculated β resonance integral value for σ overlap between the 2p orbitals of two C atoms with their distance **r** (ref. 25). The $\beta = \kappa r^2$ equation implies that a different β value is associated to any given value of the reaction coordinate r_C corresponding to the transition state relative to the attack of **E+** on each position of pyrrole. For

the attack on its α carbons, the reaction coordinate corresponding to the relevant transition state is given by r_{C1} and the relative stabilization energy is expressed by $\beta_1 = \kappa r_{C1}^2$. For attack on its β centers, the reaction coordinate of the corresponding transition state is taken as r_{C2} and the relative stabilization energy is expressed by $\beta_2 = \kappa r_{C2}^2$.

It follows that the activation barriers for the attack of E^+ on the α and β carbons of pyrrole can be expressed respectively by :

$$E_1^* = E_{C1} - \beta_1 \quad (1a); \qquad E_2^* = E_{C2} - \beta_2 \quad (1b)$$

where : $E_{C1} = nG/(m+n)$; $E_{C2} = n(G+\delta)/(m'+n)$;
and: $\beta_1 = \kappa G^2/(m+n)^2$; $\beta_2 = \kappa(G+\delta)^2/(m'+n)^2$.

Therefore, the difference between the activation barriers for the two competing paths is given by :

$$E_2^* - E_1^* = \kappa G^2/(m+n)^2 - \kappa G^2/(m'+n)^2 + nG/(m'+n) - nG/(m+n) - 2\kappa G\delta/(m'+n)^2 + n\delta/(m'+n) - \kappa\delta^2/(m'+n)^2 \quad (2)$$

This is a parabolic equation, which can be reduced to the following linear one under the reasonable assumption that $m = m'$:

$$E_2^* - E_1^* = -2\kappa G\delta/(m+n)^2 + n\delta/(m+n) - \kappa\delta^2/(m+n)^2 \quad (3)$$

Support to this assumption can be found in the observation that configurations II and III as well as their corresponding α and β heteroarenium intermediates are characterized by the same stability order.

Since : $$\log(k_2/k_1) = \log(A_2/A_1) - (E_2^* - E_1^*)/2.303RT \quad (4)$$

then: $$\log(k_2/k_1) = \log(A_2/A_1) + 35.71\delta G/(m+n)^2 + 17.85\delta^2/(m+n)^2 - 16.94n\delta/(m+n) \quad (5)$$

if T = 298 K and the energy parameters are expressed in eV.

For competing electrophilic attack of E^+ on the unencumbered α and β centers of pyrrole, we may assume in the first approximation that $A_2 = A_1$, so that :

$$\log(k_2/k_1) = 35.71\delta G/(m+n)^2 + 17.85\delta^2/(m+n)^2 - 16.94n\delta/(m+n) \quad (6)$$

As indicated before, the G term can be estimated from the $IP_V(Nu:) - EA_V(E^+)$ difference, where $IP_V(Nu:)$ refers to the vertical ionization potential of the formally localized π C_α=C_β bond of the pyrrole molecule, whereas $EA_V(E^+)$, whose values are not available from the literature, can be roughly estimated as equal to $IP_a(E\cdot)$. A Linear Combination of Bonding Orbitals (LCBO) analysis of the UV photoelectron spectrum of pyrrole allows to assign a value of *ca.* 10 eV for the vertical ionization potential of its localized π C_α=C_β bonds. By combining this value with the available $IP_a(E\cdot)$ data, the G energy gap for each of the selected ionic electrophiles can be derived. Figure 9 and 10 report correlations between the estimated G values for any given electrophile and its positional selectivity ($\log(k_2/k_1) = \log(\beta/\alpha)$)toward pyrrole (Fig. 9) and N-methylpyrrole (Fig. 10). According to the approximate eq. 6, a linear dependence of $\log(\beta/\alpha)$ on the G values is found, obeying the following equations :

$$\log(\beta/\alpha) = 0.311G - 0.454; \text{ (corr. coeff. = 0.894) for pyrrole;} \quad (7)$$
$$\log(\beta/\alpha) = 0.204G - 0.324; \text{ (corr. coeff. = 0.732) for N-methylpyrrole.} \quad (8)$$

For each pyrrolic substrate, comparison between the best-fit linear correlation of Figs. 9 and 10 and the theoretical expression 6 allows an estimate of the δ and n parameters, once a reasonable

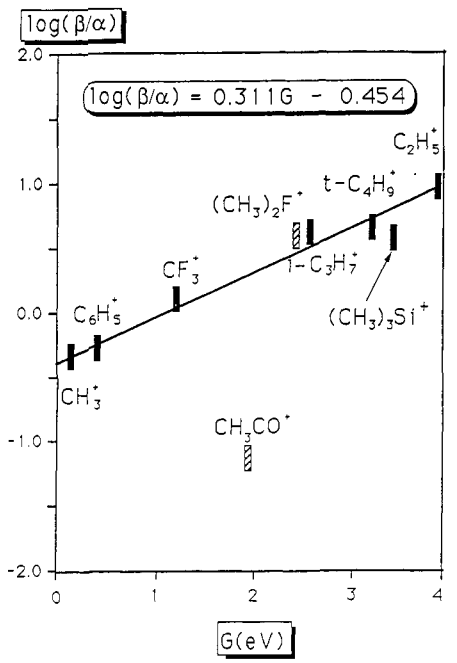

Fig. 9. Plot of site selectivity of ionic electrophiles toward the β and α carbons of pyrrole, expressed by the log(β/α), as a function of calculated **G** values.

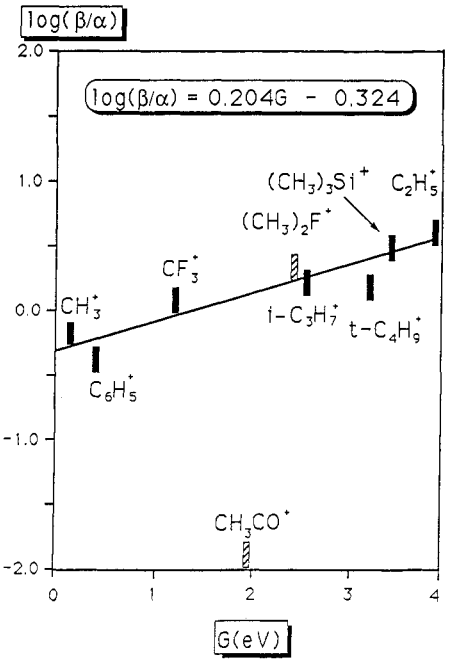

Fig. 10. Plot of site selectivity of ionic electrophiles toward the β and α carbons of N-methylpyrrole, expressed by the log(β/α), as a function of calculated **G** values.

value is attributed to the **m** term. This can be obtained by assuming the same σ C(ring)-C(alkyl) bond energy (*ca.* 87 kcal mol^{-1}) and equilibrium length (*ca.* 1.55 Å) for either α– and β–substituted heteroarenium intermediates. This leads to a value of **m** = 1.48 eV $Å^{-1}$, from which δ = 1.42 kcal mol^{-1} and **n** = 1.18 eV $Å^{-1}$ for pyrrole and δ = 1.08 kcal mol^{-1} and **n** = 1.38 eV $Å^{-1}$ for N-methylpyrrole can be derived. It is interesting to point out that similar **n** values for both pyrroles are obtained which approach closely the estimated **m** parameter. Besides, the order of magnitude of the positive δ energy gap values well compares with the relative stability of α– and β–substituted heteroarenium intermediates.

The Performance of the Curve Crossing Model. It is worthwhile to discuss from a general point of view the performance of the Curve Crossing model in predicting some outstanding features of pyrrole reactivity in the gas phase. A first important aspect arising from inspection of Fig. 4 is the reversal of site selectivity in passing from ionic electrophiles with low-lying LUMO's, *e.g.* the CH_3^+ ion, to ionic reactants with high-lying LUMO's, *e.g.* the bridged $C_2H_5^+$ cation, through rather unselective cations with borderline LUMO's, such as CF_3^+. In the framework of the Curve Crossing model, such a selectivity reversal appears as an immediate consequence of the substantially different **G** values estimated for the corresponding electrophiles. Figure 11 visualizes the effect of **G** in determining the relative magnitude of E_α^* *vs.* E_β^*, as well as the relative position of the corresponding transition states along the reaction coordinate **r**. Accordingly, low-**G** electrophiles, *e.g.* CH_3^+, are characterized by $E_\alpha^* < E_\beta^*$ and by early transition states, whereas high-**G** reactants, *e.g.* bridged $C_2H_5^+$, exhibit late transition states with $E_\alpha^* > E_\beta^*$. For borderline-**G** species, such as CF_3^+, $E_\alpha^* \simeq E_\beta^*$ as a consequence of the intermediate position of the relevant transition states along the reaction coordinate **r**. Furthermore, for each given electrophile, the transition state for β substitution on pyrroles is invariably predicted to be late relative to that governing α substitution. This may involve a less favourable activation entropy factor for β attack, which is somewhat reflected in the experimental $A_\alpha > A_\beta$ values obtained from the Arrhenius plots of Fig. 2.

In this connection, the CH_3CO^+ ion, whose **G** value can be estimated as *ca.* 1.95 eV, is expected to show a site selectivity toward pyrroles ranging around $\log(\beta/\alpha)$ = *ca.* 0.15. As a matter of fact, the experimental $\log(\beta/\alpha)$ is invariably below -1.1 for pyrroles, which implies a large deviation from the curves of Figs. 9 and 10. As previously pointed out, similar deviations from the $\log(\beta/\alpha)$ *vs.* ε(LUMO) relationship of Fig. 4 were observed for acylium ions. No reasonable explanation of such deviations could be provided by Klopman's Charge and Frontier Orbital Control model, which conceives the description of reactivity in terms of the properties of the *unperturbed* donor-acceptor pair. On the other hand, in view of the aptitude of the more refined Curve Crossing model to describe reactivity in terms of configuration mixing along the entire reaction coordinate, it was hoped that this model could comprehend the reactivity properties of CH_3CO^+ toward pyrrole. However, such an expectation seems frustrated by the present results, which confirm previous indications of a mechanistic changeover of CH_3CO^+ toward pyrroles from the classical donor-acceptor S_E2 mechanism, followed by all the other electrophiles studied, to a two-steps mechanistic sequence involving a first single electron transfer (SET) step followed by recombination of the ensuing radicals. A plausible rationale for such a peculiar mechanistic changeover for CH_3CO^+ toward pyrroles just resides in its particular **G** = *ca.* 1.95 eV value, reflecting a $\mathbf{IP_V(pyrrole) - EA_V(CH_3CO^+)}$ difference approaching zero. It follows that, along the reaction coordinate, energy degeneracy between pyrrole and CH_3CO^+ is readily reached at even limited mutual perturbation of the reactants so that a rapid SET event may occur from the donor to the acceptor *well before their interacting configurations become degenerate, as requested by the classical donor-acceptor S_E2 process*. This conclusion can be taken as a general warning, when applying Curve Crossing model to predict the reactivity of a donor-acceptor pair for which a SET event is made highly likely relative to the competing two-electrons substitution mechanism by the specific electronic features of the reactants.

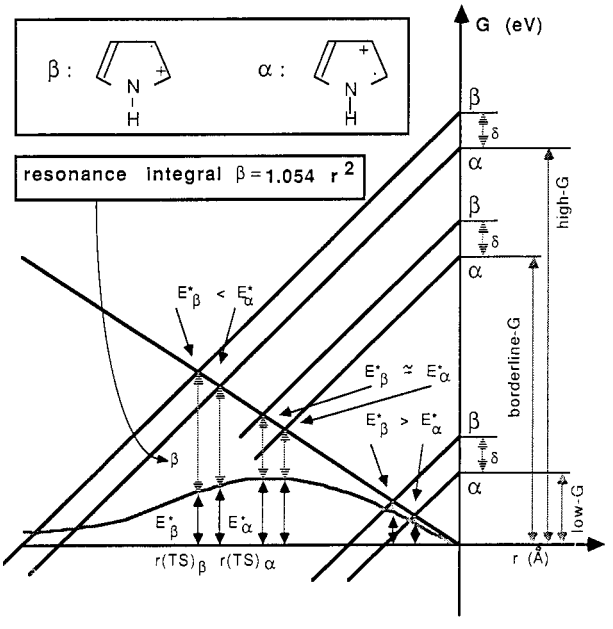

Fig. 11 State correlation diagram for a **Nu:/E⁺** donor--acceptor reaction representing a typical gas-phase heteroaromatic substitution by an ionic electrophile **E⁺**. Effect of the **G** value on the nature of the transition states and the relative height of the activation barriers involved in the attack of **E⁺** on the β and α positions of pyrrole.

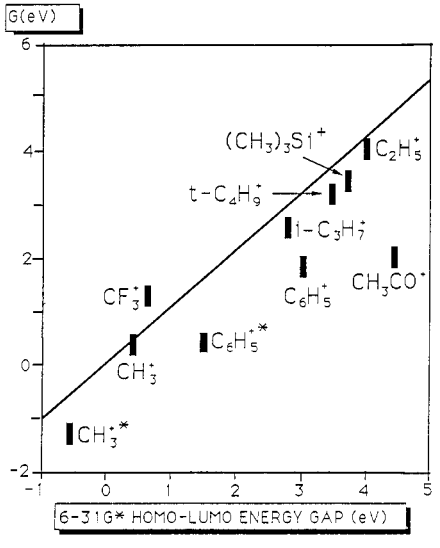

Fig. 12. Plot of the **G** values *vs.* the SCF 6-31G* calculated HOMO-LUMO energy gap for the attack of ionic electrophiles on pyrrole.

The treatment of the positional selectivity data of $(CH_3)_2F^+$ toward pyrroles within the framework of Klopman's model (Fig. 4) appears to be rather inadequate. However, an attempt to insert these data into the $\log(\beta/\alpha)$ vs. G correlations obtained by quantitative application of the Curve Crossing approach was at first glance rather promising. In fact, a rough estimate of *ca.* 2.6 eV for the G value of $(CH_3)_2F^+$ can be obtained, by taking for EA_v ($(CH_3)_2F^+$) the $-\Delta H°$ of the following reaction:

$$(CH_3)_2F^+ + e \longrightarrow CH_3F + CH_3\cdot \qquad -\Delta H° = 7.4 \text{ eV molecule}^{-1}. \qquad (9)$$

Even by using such an approximate G value, a good fitting of the $(CH_3)_2F^+$ positional selectivity as a function of the G parameter emerges (Figs. 7 and 8). However, this coincidence is fortuitous, as suggested by the peculiar Arrhenius plot of $(CH_3)_2F^+$ ions toward pyrrole (Fig. 2). In fact, the kinetic parameters order controlling the gas-phase attack of $(CH_3)_2F^+$ ions toward pyrrole, *i.e.* $E_\alpha^* < E_\beta^*$ and $A_\alpha < A_\beta$, is opposite with respect to that characterizing all other electrophiles employed. This evidence can be taken as a major indication against indiscriminate extension of the assumptions adopted in the previous section for quantitative Curve Crossing treatment of heteroaromatic reactivity. In fact, within these assumptions, $E_\alpha^* > E_\beta^*$ and $A_\alpha > A_\beta$ trends would be expected for $(CH_3)_2F^+$, (G = *ca.* 2.6 eV), as actually obtained for i-$C_3H_7^+$ (G = 2.64 eV). On these grounds, it can be concluded that, for ionic electrophiles, such as $(CH_3)_2F^+$, whose mode of attack on pyrrole cannot be regarded as a simple addition process, such as for free carbenium ions, but rather as a nucleophilic displacement process, a more refined quantitative use of the model is required, which takes into account the fact that the relevant activation barrier can arise not only by bond formation between pyrrole and the C center of the electrophile, but also by bond breaking between the outcoming methyl group and the CH_3F moiety of the electrophile.

CONCLUSIONS

A comparison between the performance of Klopman's Charge and Frontier Orbital Control concept and the Curve Crossing model, quantitatively applied for the kinetic analysis of the gas-phase attack of a number of cations on pyrroles has been presented in this study. In the framework of the first model, the experimental intramolecular selectivity is rationalized in terms of the HOMO-LUMO gap between the *unperturbed* molecules of the pyrrole donor and of the ionic acceptor. On the other hand, a better description of the experimental kinetic data is provided by the more refined Curve Crossing Model, *which builds the entire potential energy profile by allowing mixing of the appropriate electronic configurations, along the reaction coordinate.* Accordingly, for a typical donor-acceptor reaction, such as those reported in the present investigation, the activation barriers originate by the combination of two factors: i) the initial energy separation, G, between the *unperturbed* reactant and product configurations, which determines the transition state position along the reaction coordinate, and ii) the extent of configuration mixing at the transition state, which is in turn determined by the same G value. It is interesting to point out that an approximate linear correlation does exist between the G energy gap and the ε(LUMO) (E^+) - ε(HOMO) (**Pyrrole**) difference for each given electrophile, which is shown in Figure 12. On the grounds of this observation, we are inclined to conclude that Klopman's approach to the description of the gas-phase reactivity of pyrrole toward electrophiles can be thought as included in the more general Curve Crossing model. In this view, the initial HOMO(donor)-LUMO(acceptor) energy gap introduced in the former model can be interpreted, through G, as a function of physically more meaningful quantities, such as the vertical ionization potential of the donor and the vertical electron affinity of the acceptor.

Acknowledgements

I acknowledge with gratitude the contribution of my collegues and co-workers whose names appear in the references. I wish also to thank F. Cacace for his deep interest in this work and for constructive comments. Acknowledgment is also due to the Ministero della Ricerca Scientifica e Tecnologica (MURST) and the Consiglio Nazionale delle Ricerche (CNR) of Italy for financial support.

REFERENCES

1. For comprehensive reviews, see : a) G. Marino, *Adv. Heterocycl. Chem.*, *13*, 235 (1971); b) A.R. Katritzky and J.M. Lagowsky, "*The Principles of Heterocyclic Chemistry*", Academic Press, New York (1978); c) A. Albert, "*Heterocyclic Chemistry*", 2nd ed., Oxford University Press, New York (1968); d) R.A. Jones, *Adv. Heterocycl. Chem.*, *11*, 383 (1970).
2. a) R.M. Acheson, "*An Introduction to the Chemistry of Heterocyclic Compounds*", 2nd ed., Wiley, New York (1967); b) J.D. Robert and M.C. Caserio, "*Basic Principles of Organic Chemistry*", W.A. Benjamin, New York (1964); c) L.A. Paquette, "*Principles of Modern Heterocyclic Chemistry*", W.A. Benjamin, New York (1968).
3. M. Speranza, *Adv. Heterocycl. Chem.*, *40*, 25 (1986).
4. a) F. Cacace, *Radiat. Phys. Chem.*, *20*, 99 (1982); b) F. Cacace, in "*Structure/ Reactivity and Thermochemistry of Ions*", P. Ausloos and S.G. Lias, eds., D. Reidel: Dordrecht, Holland (1987); c) S.G. Lias, in "*Interactions between Ions and Molecules*", P. Ausloos, ed., Plenum, New York (1975); d) F. Cacace, *Acc. Chem. Res.*, *21*, 215 (1988).
5. G. Laguzzi, R. Bucci, F. Grandinetti, and M. Speranza, *J. Amer. Chem. Soc.*, *112*, 3064 (1990).
6. G. Laguzzi and M. Speranza, *J. Chem. Soc. Perkin Trans. 2*, 857 (1987).
7. A. Margonelli and M. Speranza, *J. Chem. Soc. Perkin Trans. 2*, 1491 (1983).
8. M.E. Crestoni, S. Fornarini, and M. Speranza, *J. Amer. Chem. Soc.*, *112*, 0000 (1990).
9. a) G. Angelini, C. Sparapani, and M. Speranza, *J. Amer. Chem. Soc.*, *104*, 7084 (1982); b) G. Angelini, G. Lilla, and M. Speranza, *ibid.*, 7091 (1982).
10. R. Bucci, G. Laguzzi, M.L. Pompili, and M. Speranza, *J. Amer. Chem. Soc.*, submitted.
11. A. Filippi, G. Occhiucci, C. Sparapani, and M. Speranza, *Can. J. Chem.*, submitted.
12. a) F. Cacace, *Adv. Phys. Org. Chem.*, *8*, 79 (1970); b) F. Cacace, *Adv. Chem. Ser.*, *197*, 33 (1981); c) M. Speranza, *Gazzetta*, *113*, 37 (1983); d) F. Cacace and M. Speranza, in "*Techniques for the Study of Ion Molecules Reactions*",J.M. Farrar and W. Saunders, Jr., eds., Wiley, New York (1988).
13. S. Wexler, in "*Actions Chimiques et Biologiques des Radiations*", M. Haissinsky, ed., Paris (1965).
14. a) J.E. Williams, Jr., V. Buss, L.C. Allen, P.v.R. Schleyer, W.A. Lathan, W.J. Hehre, and J.A. Pople, *J. Amer. Chem. Soc.*, *93*, 6867 (1971); b) J. Burdon, D.W. Davies, and G. del Conde, *J. Chem. Soc. Perkin Trans. 2*, 1193 (1976); c) J.D. Dill, P.v.R. Schleyer, J.S. Binkley, R. Seeger, J.A. Pople, and E. Haselbach, *J. Amer. Chem. Soc.*, *98*, 5428 (1976); d) P.v.R. Schleyer, A.J. Kos, and K. Ragavachari, *J. Chem. Soc. Chem. Commun.*, 1296 (1983).
15. A. Filippi, G. Occhiucci, and M. Speranza, *Can. J. Chem.*, submitted.
16. G. Angelini, C. Sparapani, and M. Speranza, *J. Amer. Chem. Soc.*, *112*, 3060 (1990).
17. J.S. Binkley, R.A. Witheside, R. Krishnan, R. Seeger, D.J. DeFrees, II.B. Schlegel, S. Topiol, L.R. Khan, and J.A. Pople, *QCPE*, *13*, 406 (1981).
18. P.C. Hariharan and J.A. Pople, *Theor. Chim. Acta*, *28*, 213 (1973).
19. a) T. Su and M.T. Bowers, *Int. J. Mass Spectrom. Ion Phys.*, *12*, 347 (1973); b) T. Su, E.C.F. Su, and M.T. Bowers, *J. Chem. Phys.*, *69*, 2243 (1978).
20. a) G. Klopman, *J. Amer. Chem. Soc.*, *90*, 223 (1968); b) R.G. Pearson, *Proc. Natl. Acad. Sci. USA*, *83*, 8440 (1986).
21. M. Shiotani, Y. Nagata, M. Tasaki, J. Sohma, and T. Shida, *J. Phys. Chem.*, *87*, 1170 (1983).
22. a) S.S. Shaik, *J. Amer. Chem. Soc.*, *103*, 3692 (1981); b) A. Pross and S.S. Shaik, *Acc. Chem. Res.*, *16*, 361 (1983); c) S.S. Shaik, *Progr. Phys. Org. Chem.*, *15*, 197 (1985); d) A. Pross, *Adv. Phys. Org. Chem.*, *21*, 99 (1985).
23. L. Libit and R. Hoffmann, *J. Amer. Chem. Soc.*, *96*, 1370 (1974), and references therein.
24. a) L. Salem, C. Leforestier, G. Segal, and R. Wetmore, *J. Amer. Chem. Soc.*, *97*, 479 (1975); b) N.D. Epiotis, "*Theory of Organic Reactions*", Springer-Verlag, Heidelberg (1978).
25. I. Fleming, "*Frontier Orbitals and Organic Chemical Reactions*", Wiley, New York (1976).